

PACS numbers: 42.65.Ky; 42.55.Vc; 32.80.Fb
DOI: 10.1070/QE2014v044n05ABEH015436

On the possibility of the generation of high harmonics with photon energies greater than 10 keV upon interaction of intense mid-IR radiation with neutral gases

A.S. Emelina, M.Yu. Emelin, M.Yu. Ryabikin

Abstract. **Based on the analytical quantum-mechanical description in the framework of the modified strong-field approximation, we have investigated high harmonic generation of mid-IR laser radiation in neutral gases taking into account the depletion of bound atomic levels of the working medium and the electron magnetic drift in a high-intensity laser field. The possibility is shown to generate high-order harmonics with photon energies greater than 10 keV under irradiation of helium atoms by intense femtosecond laser pulses with a centre wavelength of 8–10.6 μm.**

Keywords: *mid-IR lasers, atoms, ionisation, high harmonic generation, X-rays.*

1. Introduction

The past few years have seen a significant progress in the development of high-power femtosecond parametric lasers of near and mid-IR ranges. Different types of laser sources generating pulses with energy of the order of millijoules or higher have been designed; the centre wavelengths of these sources lie in the range 1.5–4 μm [1–3]. Fabrication of such sources opens new avenues in studying the interaction of high-intensity laser radiation with matter. One of the areas of research, where these possibilities manifest themselves most significantly [4–9], is the physics of the processes associated with the rescattering of electrons [10, 11] under tunnelling ionisation. Such processes include, in particular, high-order harmonic generation (HHG) of laser radiation [12, 13].

An important characteristic of various processes caused by the ionisation of gases by intense laser radiation is the average energy U_p of electron oscillations in an alternating electric field with the amplitude E and frequency ω:

$$U_p = \frac{e^2E^2}{4m\omega^2} \sim I\lambda^2, \quad (1)$$

where e and m are the electron charge and mass; and I and λ are the intensity and wavelength of laser radiation. The value of U_p determines, in particular, the high-energy boundary of the plateau-shaped distribution in the HHG spectrum of gases; the position of this boundary is given by a universal expression [11, 14]

$$\hbar\Omega_{max} \approx I_p + 3.17U_p, \quad (2)$$

where I_p is the ionisation potential of an atom.

Proportionality of the electron quiver energy U_p to the square of the laser radiation wavelength indicates the principle possibility of a significant expansion of the plateau in the HHG spectrum to the high-frequency region [4, 15] when use is made of mid-IR sources. This possibility has been vividly demonstrated in a recent experiment [5], where the ionisation of helium atoms by the radiation of a laser [2] with the centre wavelength $\lambda = 3.9$ μm was accompanied by the emergence of a coherent broadband supercontinuum with a maximum energy of photons reaching 1.6 keV.

The HHG experiments [5] with a radiation source at $\lambda = 3.9$ μm were carried out at a relatively low (3.3×10^{14} W cm^{-2}) peak intensity of the laser pulses. This intensity is only slightly above the ionisation threshold of helium and was selected based on the condition of the smallness of the concentration of plasma produced by ionisation of helium, which allows the phase-matched generation [16, 17] to obtain ultrabright HHG radiation in a capillary filled with a gas under high pressure. At the same time, of great interest is the issue of the maximum achievable spectral HHG width, which in principle (with the proper solution of the problem of phase-matching or quasi-phase-matching) can be obtained by using mid-IR sources.

For a given wavelength of the laser source the width of the plateau in the HHG spectrum, according to (1), (2), can in principle be increased by increasing intensity of the laser radiation. However, one of the major limiting factors here is the depletion of atomic levels at high intensities of the incident radiation; this effect leads to a decrease in the yield of harmonics and cessation of growth of the spectral HHG width at intensities that significantly exceed the ionisation threshold [18, 19]. Another factor that may limit the generation efficiency of harmonics and their maximum energy at high laser intensities is the influence of the magnetic field of laser radiation. This influence manifests itself in deviation ('magnetic drift') of trajectories of electrons moving with subrelativistic velocities from straight lines and, as a result [20–22], causes a reduction of the effectiveness of the HHG mechanism which is based on the collision of electrons with their parent ions. In the course of interaction of visible or near-IR radiation with

A.S. Emelina, M.Yu. Emelin, M.Yu. Ryabikin Institute of Applied Physics, Russian Academy of Sciences, ul. Ul'yanova 46, 603950 Nizhnii Novgorod, Russia; N.I. Lobachevsky Nizhnii Novgorod State University (National Research University), prosp. Gagarina 23, 603905 Nizhnii Novgorod, Russia; e-mail: ana_b@rambler.ru, emelin@ufp.appl.sci-nnov.ru, mike@ufp.appl.sci-nnov.ru

Received 3 March 2014
Kvantovaya Elektronika **44** (5) 470–477 (2014)
Translated by I.A. Ulitkin

neutral atoms, this factor is not important because the speed of a free electron under the intensities at which atoms are ionised is in these cases much less than the speed of light. However, it should be expected that, in view of the above scaling of the electron quiver energy (1), the influence of this factor when use is made of long-wavelength sources can be significant even at moderate peak intensities of laser pulses.

Simultaneous consideration of these factors is important both for understanding their relative role in the HHG process under different conditions and for formulating general conclusions about the limits of ability to generate high-energy photons during the HHG of laser radiation in gases. Our preliminary studies [23] in this direction were based on numerical calculations in a single-active-electron approximation [14, 24], using a two-dimensional model of the atom. These calculations, performed outside the scope of the electric dipole approximation, demonstrated the possibility of obtaining high-order harmonics in noble gases, with maximum energies (depending on a particular atom) of about 1–7 keV at $\lambda = 3.9$ μm. In thses cases, the generation of high-order harmonics can be largely suppressed due to the influence of the magnetic field of the laser pulse, and the maximum width of their spectrum is mainly determined by the effect of the depletion of atomic levels.

For more realistic three-dimensional calculations and for consideration of HHG in a wider range of laser radiation and working gas medium parameters, we developed an analytical description of the process [25]. This description is based on the most widely used analytical theory of high harmonic generation – Lewenstein's theory [26], modified so as to take into account the above two factors limiting the HHG process. For atoms and ions with different ionisation potentials (hydrogen and helium atoms and a helium ion with ionisation potentials I_p equal, respectively, to 13.6, 24.6 and 54.4 eV) using the analytical approach developed in [25] we evaluated the achievable limits of the width of the HHG spectrum taking into account the limiting effects; the calculations were performed for laser sources with wavelengths $\lambda = 0.8–3.9$ μm. For a helium ion in the radiation field with $\lambda = 3.9$ μm we showed the possibility of generating high-order harmonics with energies up to 30 keV. In this case, both the restrictions on the width of the spectrum of the harmonics and on the efficiency of their generation are mainly caused by the factor related to the electron magnetic drift; the intensity distribution in the HHG spectrum in this case acquires, instead of a plateau-like shape, an arc-like one with an intensity peak in the photon energy region of 15 to 20 keV.

Thus, it follows from the above calculations that the use of radiation of a recently designed femtosecond source with $\lambda = 3.9$ μm [2] enables the generation of high harmonics with energies of tens of kiloelectronvolts under irradiation of ions. However, it should be noted that in the HHG experiments neutral gases are preferable, and the intensity of the laser pulses should not greatly exceed the ionisation threshold of the atoms so that the concentration of the resultant plasma remained relatively low, which would reduce the influence of undesirable effects caused by the dispersion of the electromagnetic waves and defocusing of the laser beam in the plasma. In this regard, urgent is the task of searching for the optimal conditions for efficient generation of high-energy photons during the HHG process in neutral gases. In this paper we have investigated the feasibility of using for this purpese an intense mid-IR laser radiation with the centre wavelength $\lambda \approx 10$ μm.

2. Analytical description

The theoretical approach used in this paper is based on the modification [25] of the analytic HHG theory developed by Lewenstein and co-authors.

Lewenstein's theory [26] (see also [27]) is a quantum-mechanical generalisation of the semiclassical model [11], which gave the explanation of the mechanism and main properties of high harmonic generation in gases. In the semiclassical model [11], the HHG is considered as a three-step process consisting of a tunnelling detachment of the electron from the atom, its motion in an oscillating electric field and return to the parent ion with the emission of a high-energy photon. In Lewenstein's theory, use is made of a single-active-electron approximation; the electron wave function in the framework of this theory can be represented as a superposition of the unperturbed eigenfunction of the bound ground state in the atom and a set of functions of a continuum, which, in accordance with the strong-field approximation, have the form of plane waves, excluding the effect of the Coulomb potential. The time-dependent mean dipole moment of the system is expressed by the integral over time and components of the canonical momentum of the electron containing a rapidly oscillating integrand factor in the form of an exponent whose factor represents a semiclassical action of the electron $S(\boldsymbol{p}, t, t')$ ($\boldsymbol{p}$ is the canonical momentum of the electron, t is the current time and t' is a temporary variable of integration). The main contribution to the integrals in the momentum is given by the stationary points of the action: $\nabla_{\boldsymbol{p}} S(\boldsymbol{p}, t, t') = 0$. These points, on the one hand, greatly simplify the calculations, allowing the use of the method of stationary phase. On the other hand, these stationary points have a clear physical meaning: Their contribution to the high-frequency nonlinear response of the system corresponds to free electron trajectories starting at the nucleus and ending in it at a later time; this situation corresponds to the assumptions of the semiclassical theory [11]. Thus, the quantum-mechanical theory [26] has made it possible to maintain the clarity of the semiclassical model and confirmed its main conclusions, by providing the opportunity to include purely quantum effects such as tunnelling and quantum interference in the description.

In our paper [25] Lewenstein's theory has been modified so that it has become possible to describe simultaneously the effect of depletion of the atomic levels and electron magnetic drift. It should be noted that in previous HHG studies analytical approaches considered separately the influence of the magnetic field of the laser pulse [22, 28, 29] and the depletion of the ground state of the atom or molecule [26, 30, 31]. The approach developed in [25] takes account of these two factors simultaneously. The expression [25] for the alternating dipole moment of an atom in an external linearly polarised electromagnetic field has the form (hereinafter, atomic units are used):

$$
\begin{aligned}
x(t) = \mathrm{i}\int_0^\infty \mathrm{d}\tau \left(\frac{\pi}{\varepsilon + \mathrm{i}\tau/2}\right)^{3/2} d_x^*(\boldsymbol{p}_{\mathrm{st}}(t,\tau) - \boldsymbol{A}(t)) \\
\times d_x(\boldsymbol{p}_{\mathrm{st}}(t,\tau) - \boldsymbol{A}(t-\tau)) E(t-\tau) \\
\times \exp\left[-\mathrm{i}S(p_{\mathrm{st}x}, t, \tau) - \mathrm{i}S_{\mathrm{m}}(\boldsymbol{p}_{\mathrm{st}}, t, \tau) - \int_0^t \frac{W(t')}{2}\mathrm{d}t' \right. \\
\left. - \int_0^{t-\tau} \frac{W(t')}{2}\mathrm{d}t'\right] + \text{c.c.}
\end{aligned}
\tag{3}
$$

Here, $E(t)$ and $A(t)$ are the electric field and vector potential of the laser pulse, respectively; τ is the time of electron motion in free space; ε is the regularisation parameter, which can be chosen small; $d_x(\boldsymbol{p})$ is the x-component of the dipole matrix element corresponding to the transition from the bound ground state to the continuum; in considering the helium atom in a single-active-electron approximation, for the matrix element we use the same expression as for hydrogen-like atoms:

$$d_x(\boldsymbol{p}) = \mathrm{i}\frac{2^{7/2}(2I_\mathrm{p})^{5/4}}{\pi}\frac{p_x}{(\boldsymbol{p}^2+2I_\mathrm{p})^3}; \quad (4)$$

$S(p_x,t,\tau)$ is the quasi-classical action describing the free motion of an electron in the laser pulse field, excluding the effect of the magnetic field:

$$S(p_x,t,\tau) = \int_{t-\tau}^{t}\left\{\frac{1}{2}\left[p_x - \frac{A(t')}{c}\right]^2 + I_\mathrm{p}\right\}\mathrm{d}t'; \quad (5)$$

$S_\mathrm{m}(\boldsymbol{p},t,\tau)$ is the correction (found similarly to [22]) to the action resulting from the expansion of the vector potential $\boldsymbol{A}(t - z/c)$ in a series over the coordinate of laser radiation propagation (we restrict ourselves to the linear term of this expansion, giving the correction of the first order in $\dot{x}/c$ to $\boldsymbol{A}(t)$ in the electric dipole approximation, which, in the case of long-wavelength laser radiation, is sufficient to adequately take into account the effect of the magnetic field [20]); in the case of a laser pulse linearly polarised along the x axis, which propagates in the direction of the z axis, the correction to the action has the form

$$S_\mathrm{m}(\boldsymbol{p},t,\tau) = \int_{t-\tau}^{t}\frac{1}{2}\left\{p_z - \left[\frac{p_x A(t')}{c^2} - \frac{A^2(t')}{2c^3}\right]\right\}^2\mathrm{d}t'; \quad (6)$$

$\boldsymbol{p}_\mathrm{st}(t,\tau)$ is a stationary canonical momentum of an electron, corresponding to the trajectory starting in the nucleus at an instant $t-\tau$ and ending in it at the instant t, with the components

$$p_{\mathrm{st}x}(t,\tau) = \frac{1}{\tau}\int_{t-\tau}^{t}\frac{A(t')}{c}\mathrm{d}t', \quad (7)$$

$$p_{\mathrm{st}z}(t,\tau) = \frac{p_{\mathrm{st}x}^2}{c} - \frac{1}{2c\tau}\int_{t-\tau}^{t}\frac{A^2(t')}{c^2}\mathrm{d}t'. \quad (8)$$

Integrand factors $d_x(\boldsymbol{p}_\mathrm{st}(t,\tau) - \boldsymbol{A}(t-\tau))E(\mathrm{t}-\tau)$ and $d_x^*(\boldsymbol{p}_\mathrm{st}(t,\tau) - \boldsymbol{A}(t))$ in expression (3) for the alternating dipole moment define, respectively, the amplitudes of the transition probabilities from the ground state to the continuum at an instant $t-\tau$ and from the continuum to the ground state at an instant t. Account for the depletion of the ground state of the atom is reduced to multiplication of these amplitudes by the amplitude of the ground state at instants $t-\tau$ and t. The latter can be calculated as

$$a(t) = \exp\left[-\int_0^t\frac{W(t')}{2}\mathrm{d}t'\right],$$

where $W(t)$ is the instantaneous ionisation rate of an atom. As an expression for $W(t)$, we use the expression for the static field-induced tunnelling ionisation rate of atoms, corrected for the barrier-suppression regime, proposed in [32]:

$$W(t) = C_1^2\left(\frac{4I_\mathrm{p}}{|E(t)|}\right)^{\frac{2Z}{\sqrt{2I_\mathrm{p}}}-1}\exp\left[-\frac{2(2I_\mathrm{p})^{3/2}}{3|E(t)|}\right]\exp\left[-\frac{6Z^2|E(t)|}{I_\mathrm{p}(2I_\mathrm{p})^{3/2}}\right], \quad (9)$$

where C_1^2 is a numerical coefficient, which is determined from the condition of normalisation of the wave function; and Z is the effective nuclear charge. The second exponential factor in (9) is necessary for an adequate description of the ionisation rate in the barrier-suppression regime: without it, as is well known [32, 33], the ionisation rate at large E (of interest in our study) is grossly overestimated.

Expression (3) clearly shows that each of the effects discussed here can be independently included or excluded from the calculation by inclusion or exclusion of the relevant correction factors.

3. Results of calculations

Below we present the results of calculations obtained by using the developed analytical theory. In all calculations the laser field was specified in the form of a Gaussian pulse with FWHM equal to six field cycles; the calculations were performed for a helium atom in a single-active-electron approximation.

The calculations show that for a given atomic target the dominant mechanism limiting the spectral HHG width and efficiency of the harmonic generation depends on the laser radiation wavelength λ. Figure 1 shows the HHG spectra obtained in atomic helium under conditions corresponding to the broadest possible spectrum of the generated radiation at different λ.

Spectra for $\lambda = 2$ μm, $I = 3.7\times10^{15}$ W cm^{-2} (black curve in Fig. 1a) and $\lambda = 3.9$ μm, $I = 2.35\times10^{15}$ W cm^{-2} (Fig. 1b) have the form of steps. The occurrence of these steps is due to the fact that in these examples, the peak intensity of the laser pulse is several times higher than the value corresponding to ionisation saturation of helium atoms; therefore, ionisation occurs at the leading edge of the pulse. Owing to the ionisation, the population of the ground atomic state on each half cycle of the laser field decreases, and consequently, the intensity of the generated harmonics decreases as well. At the same time, as the amplitude of the laser field at the leading edge of the pulse increases, the emission spectrum generated in collisions of electrons with the parent ions broadens with each subsequent half-cycle of the field. As a result, a harmonic spectrum is formed with an intensity distribution, qualitatively different from the case of weak ionisation [for comparison Fig. 1a shows the HHG spectrum (gray curve), calculated by neglecting the depletion of the ground state and the influence of the magnetic field]. In the presence of strong ionisation, the harmonic spectrum shown in Fig. 1b is a set of plateaus with cutoff energies corresponding to the maximum energies of the electron returning to the parent ion for the corresponding half-cycles of oscillations of the electric field of the laser pulse; the average yield of harmonics within these areas is reduced with increasing cutoff energy. With a further increase in the peak intensity of the laser pulse the width of the harmonic spectrum ceases to increase, and the yield of the generated harmonics decreases. In the cases presented in Figs 1a and 1b, the magnetic field also leads to a decrease in the intensity of the generated harmonics (by tens of percent for $\lambda = 2$ μm and by several times for $\lambda = 3.9$ μm), but due to the depletion of the ground state the HHG efficiency is many orders of magnitude smaller than when only the effect of the magnetic field is taken into account.

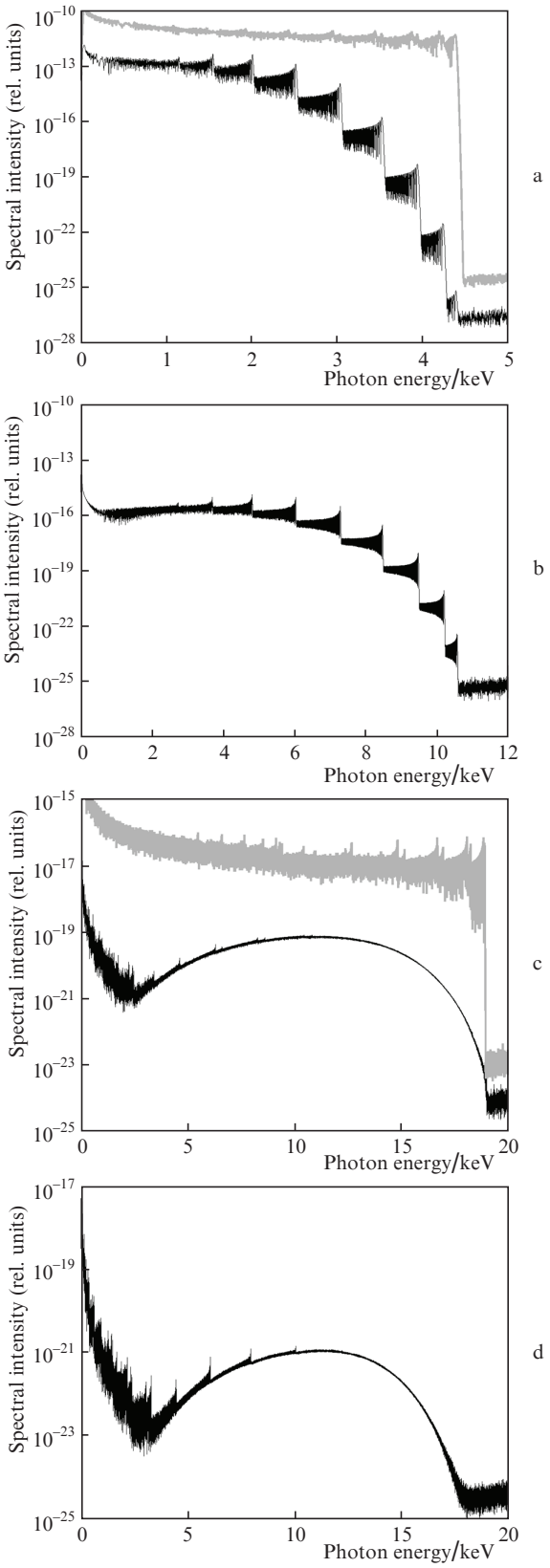

Figure 1. HHG spectra for the helium atom in the field of laser pulses (pulses with a Gaussian profile and FWHM $6T$, where T is the laser field cycle) with different centre radiation wavelengths and peak intensities: (a) $\lambda = 2$ μm, $I = 3.7 \times 10^{15}$ W cm^{-2}, (b) $\lambda = 3.9$ μm, $I = 2.35 \times 10^{15}$ W cm^{-2}, (c) $\lambda = 8$ μm, $I = 10^{15}$ W cm^{-2} and (d) $\lambda = 10.6$ μm, $I = 5.5 \times 10^{14}$ W cm^{-2}. Gray curves represent the results of calculations in the framework of Lewenstein's theory without account for the limiting factors.

Calculations for the wavelengths $\lambda = 8$ and 10.6 μm show that in the case of long-wavelength pumping, the relative role of the factors suppressing the HHG changes dramatically. This, in particular, is evidenced by the HHG spectra, which change in comparison with the case of short-wavelength pumping: the spectra in Figs 1c and 1d, instead of plateau-like structures with sharp cutoffs, exhibit smooth arc-like distributions that are typical of a situation when the magnetic drift plays a significant role in the dynamics of the electron [25, 29]. The occurrence of such distributions is associated with the consequent effect of suppression of the contributions of so-called long trajectories to the high-frequency response of the system in a strong field (see below).

The increasing role of the effects at large λ, which are caused by the influence of the magnetic field, becomes even more obvious if we consider Figs 2 and 3 demonstrating the dependence of the HHG yield on the laser intensity for the helium atom irradiated by the laser pulse ($\lambda = 8$ μm). Figure 2 shows the dependences of the integral HHG energy in the high-frequency region of the spectrum on the laser intensity, calculated in different approximations (without account for the depletion of the ground state and the influence of the magnetic field, with account for the depletion of the ground state, with account for the magnetic field and with account for both the depletion of the ground state and the magnetic field). Integration was carried out over harmonics with photon energies greater than $I_p + 0.1\Delta$, where $\Delta = 3.17U_p$ is the plateau width. These dependences indicate that at $\lambda = 8$ μm the magnetic field exerts a strong influence on the dynamics of the electron at an intensity corresponding to the ionisation threshold of helium atoms, and throughout the range of intensities, this effect is dominant in suppressing the HHG. While taking into account only the depletion of the atomic levels, the laser radiation intensity corresponding to the HHG saturation is $\sim 9 \times 10^{14}$ W cm^{-2}, and the HHG yield decreases only several-fold, whereas the account for the influence of the magnetic field leads to the fact that the saturating intensity decreases down to 7×10^{14} W cm^{-2} and the HHG yield – by more than two orders of magnitude.

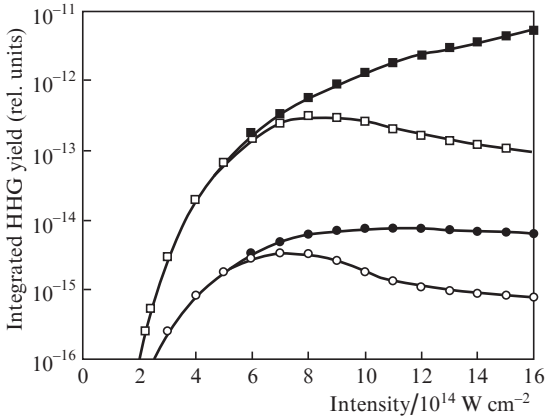

Figure 2. Integrated HHG yield with photon energies greater than $I_p + 0.1\Delta$ for the helium atom vs. the peak intensity of the laser pulse ($\lambda = 8$ μm), calculated without account for the depletion of the ground state and the influence of the magnetic field (■), as well as with account for the depletion of the ground state (□), magnetic field (●) and both the depletion of the ground state and the magnetic field (○).

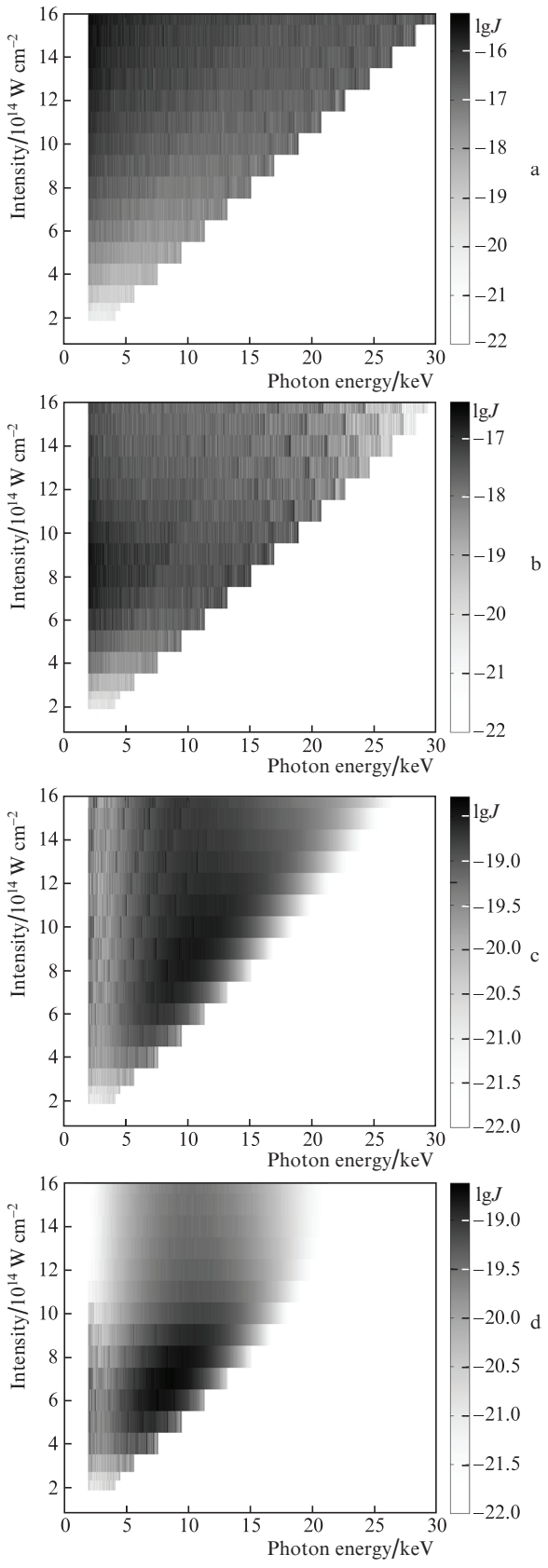

Figure 3. HHG spectra for the helium atom in the radiation field with $\lambda = 8$ μm vs. the peak intensity of a laser pulse, calculated without account for the depletion of the ground state and the influence of the magnetic field (a) as well as with account for the depeltion of the ground state (b), the magnetic field (c) and both the depletion of the ground state and the magnetic field (d) (J is the spectral intensity).

More detailed information about the relative role of the factors of HHG suppression (Fig. 3) is given by the 'contour maps' that show, as in Fig. 2, the dependences of the HHG yield on the peak laser intensity, calculated in various approximations; in contrast to Fig. 2, these dependences are presented in Fig. 3 with a resolution over the spectrum of the generated high harmonics.

According to Fig. 3a, the calculations in the framework of Lewenstein's theory without account for the limiting factors give a monotonic increase in the HHG yield with increasing intensity I; the HHG spectra have a plateau-like shape with a cutoff energy linearly increasing in accordance with the universal expression (2).

The depletion of the ground state, taken into account in the calculations whose results are shown in Fig. 3b, leads to a monotonic decrease in the HHG yield with increasing I, starting with some intensity at which the ionisation rate reaches a critical value (see also Fig. 2). The efficiency of generation of high harmonics decreases with increasing their order, which finally leads to a limitation in the spectral width of the generated harmonics (see Fig. 3b at large I).

The electron magnetic drift, taken into account in the calculations the results of which are shown in Fig. 3c, leads, as noted above, to the formation of the arc-shaped intensity distribution in the HHG spectrum: in the entire range of the intensities under study, the HHG yield has a maximum in the central region of the spectrum, while both the lower- and higher-order harmonics are strongly suppressed. This change in the HHG spectrum is due to the fact that the contributions of different types of electron trajectories to the polarisation response of the system turn out to be suppressed to a variable degree because of the electron magnetic drift [29]. In the absence of the magnetic drift the HHG signal contains contributions of short (with the time of the electron motion from the moment of detachment to the moment of the return to the parent ion, $\tau < 0.65T$, where T is the laser field cycle) and long ($\tau \geqslant 0.65T$) electron trajectories; coherent summation of the contributions of these trajectories leads to the formation of the plateau-like distribution with a clearly pronounced high-frequency cutoff and spectral interference (see, e.g., gray curves in Fig. 1). At high intensities I, corresponding to the subrelativistic regime of interaction of the electron with the laser field, the electrons experience a magnetic drift, and for trajectories with large τ this drift is greater; hence, at sufficiently large I the contributions of long trajectories are completely suppressed, and contributions of short trajectories are suppressed partially. As a result, the spectrum acquires an arc-like shape (Figs 1c and 1d), and the spectral interference of contributions from different trajectories disappears, except for the low-frequency region. With increasing laser radiation intensity the maximum of the HHG spectrum shifts towards higher energies; however, starting with some value of I, the HHG yield decreases with increasing I and the broadening of the spectrum of high-order harmonics slows down.

The calculations, the results of which are shown in Fig. 3d, demonstrate the effect of both limiting factors. In the case of atomic helium, in the radiation field with $\lambda = 8$ μm at relatively low laser intensities (from the ionisation threshold to about $I = 7 \times 10^{14}$ W cm^{-2}) the behaviour of the HHG spectrum is primarily determined by the influence of the electron magnetic drift; in this region the spectra in Figs 3c and 3d are practically identical; position of the maximum of the HHG spectrum at $I = 7 \times 10^{14}$ W cm^{-2} corresponds to about 10 keV.

At higher I, however, the depletion of the ground state begins resulting in a rapid decrease in the HHG yield with increasing I (see also Fig. 2), and the width of the spectrum is limited by the value ~18 keV.

The above-mentioned information about the contributions of different electron trajectories to the HHG signal is graphically illustrated in Fig. 4 by the signal spectrograms for helium atoms in the field of the laser pulse ($\lambda = 8$ μm, $I = 1.2 \times 10^{15}$ W cm^{-2}). Presented are the time dependences of the squares of the coefficients of the wavelet-transform of the HHG signal; the wavelet analysis was performed by the analysing function

$$T_{t_0\Omega}(t) = \sqrt{\Omega}\,\Phi(\Omega(t - t_0)),$$

where as the mother wavelet use was made of the Morlet wavelet

$$\Phi(\eta) = \frac{1}{\sqrt{\tilde{\tau}}}\exp(\mathrm{i}\eta)\exp\left(-\frac{\eta^2}{2\tilde{\tau}^2}\right)$$

(see, e.g., [34]); t_0 and Ω are the variables used respectively for shifting and scaling the wavelet-transform window; in selecting the parameter $\tilde{\tau}$ equal to $5\pi/\sqrt{2\ln 2} \approx 13.34$, the full width of the analysing function at half-maximum is equal to five cycles of the laser field. We present the results of the analysis of the HHG signal calculated in the electric dipole approximation and beyond it. In the absence of the electron magnetic drift (electric dipole approximation, Fig. 4a) the HHG signal, as noted above, contains the contributions of different types of trajectories, short trajectories corresponding to high-frequency components with a positive chirp, long ($0.65T \leqslant \tau \leqslant T$) – to high-frequency components with a negative chirp and even longer ($\tau > T$) – to low-frequency components with a positive or negative chirp. Due to the influence of the magnetic drift (calculations beyond the electric dipole approximation, Fig. 4b), the contributions of all long trajectories are completely suppressed, and of short ones – in part (the most intense is the signal in the energy range ~12 keV, which is consistent with Fig. 3d). In both cases one can see in Fig. 4 the effect of the depletion of the ground state, which manifests itself in a gradual weakening of the signal over time, resulting in asymmetrical spectrograms.

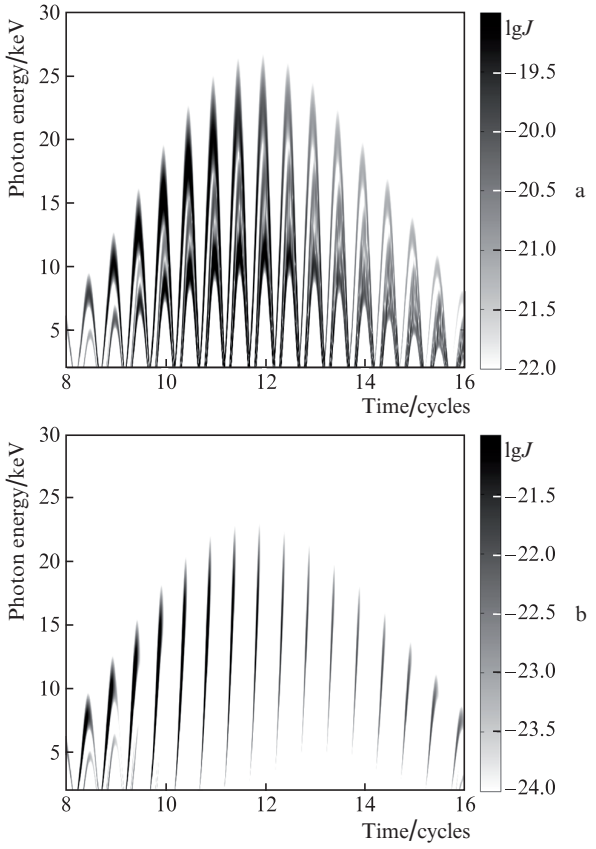

Figure 4. Spectrograms of the HHG signal for the helium atom in the field of the laser pulse ($\lambda = 8$ μm, $I = 1.2 \times 10^{15}$ W cm^{-2}), calculated (a) in the electric dipole approximation and (b) beyond it.

Figures 1d, 5 and 6 show the results of the same analysis for laser radiation with $\lambda = 10.6$ μm. In general, they are similar to the results for $\lambda = 8$ μm. It should be noted, however, that at $\lambda = 10.6$ μm the restrictions on both the HHG efficiency and the width of the HHG spectrum are almost entirely determined by the electron magnetic drift. This, in particular, is evidenced by the fact that even at $I = 2 \times 10^{14}$ W cm^{-2}, which is only slightly above the ionisation threshold of helium, the contributions of long trajectories to the HHG signal are strongly suppressed in comparison with the contribution of short trajectories (see Fig. 6a). The maximum HHG efficiency is achieved at $I \approx 5.5 \times 10^{14}$ W cm^{-2} (Fig. 5); the photon energy corresponding to this maximum is ~12 keV (see also Fig. 1d). It is important to note that under these optimal conditions, the degree of ionisation of the medium is not high, which is important from the point of view of implementation of the phase-matching conditions [16, 17] to obtain ultrabright HHG radiation in an extended medium. Even when $I = 7.5 \times 10^{14}$ W cm^{-2}, the depletion of the ground atomic state is negligible. This is confirmed by the symmetry of the spectrogram in Fig. 6b: The HHG signal generated at the trailing edge of the laser pulse is not weaker than at its leading edge.

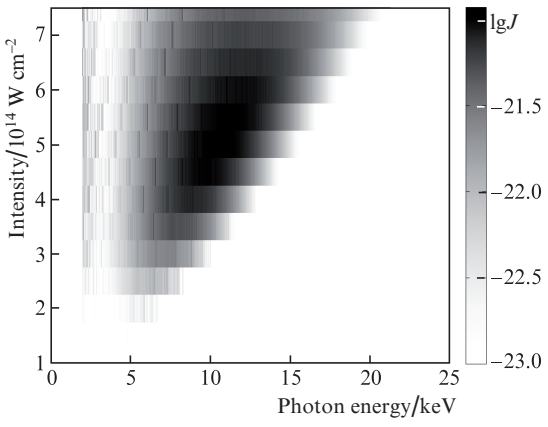

Figure 5. Same as in Fig. 3d, but for $\lambda = 10.6$ μm.

4. Conclusions

Theoretical calculations carried out in this paper allow us to elucidate the role of the factors associated with the depletion

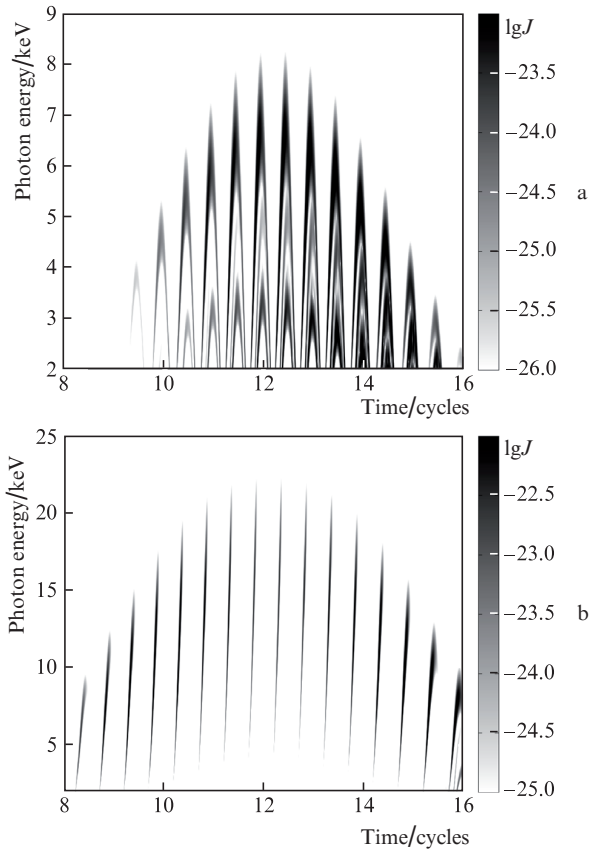

Figure 6. Same as in Fig. 4b, but for $\lambda = 10.6$ μm and $I = (a)\ 2 \times 10^{14}$ and (b) 7.5×10^{14} W cm^{-2}.

of atomic levels of the working medium and the influence of the magnetic field of the laser pulse during the HHG of mid-IR laser radiation in neutral gases and to draw conclusions about the maximum achievable energy of photons generated under these conditions. The relative role of the limiting factors is to a large extent determined by the wavelength of the laser radiation. When helium atoms are irradiated by intense femtosecond pulses with a centre wavelength of $\lambda = 2-3.9$ μm, the main limiting effect is the depletion of the bound states, while in the case of long-wavelength radiation ($\lambda = 8-10.6$ μm), the main factor of the HHG suppression is the influence of the magnetic field of the laser radiation. In the latter case we should expect the HHG with photon energies up to 20 keV with a maximum efficiency at a radiation intensity of $(5-7) \times 10^{14}$ W cm^{-2}, the energy of the most effectively generated photons reaching 10–12 keV. Results of the study are interesting from the standpoint of clarifying the prospects for creating compact sources of ultrashort pulses of coherent hard X-rays that can compete with large-scale synchrotron sources.

Acknowledgements. This work was supported by the Presidium of the Russian Academy of Sciences (Programme 'Extreme Light Fields and Their Applications'), the Russian Foundation for Basic Research (Grant No. 12-02-12101-ofi_m and 14-02-00762), the RF Ministry of Education and Science (Contract No. 11.G34.31.0011) and the RF President's Grants Council (Support to the Leading Scientific Schools Programme, Grant No. NSh-2001.2014). A.S. Emelina acknowledges the support from the Dynasty Nonprofit Foundation. The authors are grateful to the Joint Supercomputer Centre of RAS and SNIC for providing computing resources.

References

1. Schmidt B.E., Béjot P., Giguére M., Shiner A.D., Trallero-Herrero C., Bisson É., Kasparian J., Wolf J.-P., Villeneuve D.M., Kieffer J.-C., Corkum P.B., Légaré F. *Appl. Phys. Lett*., **96**, 121109 (2010).
2. Andriukaitis G., Balciunas T., Ališauskas S., Pugžlys A., Baltuška A., Popmintchev T., Chen M.-C., Murnane M.M., Kapteyn H.C. *Opt. Lett*., **36**, 2755 (2011).
3. Deng Y., Schwarz A., Fattahi H., Ueffing M., Gu X., Ossiander M., Metzger T., Pervak V., Ishizuki H., Taira T., Kobayashi T., Marcus G., Krausz F., Kienberger R., Karpowicz N. *Opt. Lett*., **37**, 4973 (2012).
4. Colosimo P., Doumy G., Blaga C.I., Wheeler J., Hauri C., Catoire F., Tate J., Chirla R., March A.M., Paulus G.G., Muller H.G., Agostini P., DiMauro L.F. *Nat. Phys*., **4**, 386 (2008).
5. Popmintchev T., Chen M.-C., Popmintchev D., Arpin P., Brown S., Ališauskas S., Andriukaitis G., Balčiunas T., Mücke O.D., Pugzlys A., Baltuška A., Shim B., Schrauth S.E., Gaeta A., Hernández-Garsía C., Plaja L., Becker A., Jaron-Becker A., Murnane M.M., Kapteyn H.C. *Science*, **336**, 1287 (2012).
6. Blaga C.I., Xu J., DiChiara A.D., Sistrunk E., Zhang K., Agostini P., Miller T.A., DiMauro L.F., Lin C.D. *Nature*, **483**, 194 (2012).
7. DiChiara A.D., Sistrunk E., Blaga C.I., Szafruga U.B., Agostini P., DiMauro L.F. *Phys. Rev. Lett*., **108**, 033002 (2012).
8. Vozzi C., Negro M., Stagira S. *J. Mod. Opt*., **59**, 1283 (2012).
9. Hernández-Garsía C., Pérez-Hernández J.A., Popmintchev T., Murnane M.M., Kapteyn H.C., Jaron-Becker A., Becker A., Plaja L. *Phys. Rev. Lett*., **111**, 033002 (2013).
10. Schafer K.J., Yang B., Krause J.L., Kulander K.C. *Phys. Rev. Lett*., **70**, 1599 (1993).
11. Corkum P.B. *Phys. Rev. Lett*., **71**, 1994 (1993).
12. McPherson A., Gibson G., Jara H., Johann U., Luk T.S., McIntyre I.A., Boyer K., Rhodes C.K. *J. Opt. Soc. Am. B*, **4**, 595 (1987).
13. Ferray M., L'Huillier A., Li X.F., Lompre L.A., Mainfray G., Manus C. *J. Phys. B: At. Mol. Opt. Phys*., **21**, L31 (1988).
14. Krause J.L., Schafer K.J., Kulander K.C. *Phys. Rev. Lett*., **68**, 3535 (1992).
15. Shan B., Chang Z. *Phys. Rev. A*, **65**, 011804(R) (2001).
16. Yakovlev V.S., Ivanov M., Krausz F. *Opt. Express*, **15**, 15351 (2007).
17. Popmintchev T., Chen M.-C., Bahabad A., Gerrity M., Sidorenko P., Cohen O., Christov I.P., Murnane M.M., Kapteyn H.C. *Proc. Nat. Acad. Sci. USA*, **106**, 10516 (2009).
18. Moreno P., Plaja L., Malyshev V., Roso L. *Phys. Rev. A*, **51**, 4746 (1995).
19. Strelkov V.V., Sterjantov A.F., Shubin N.Yu., Platonenko V.T. *J. Phys. B: At. Mol. Opt. Phys*., **39**, 577 (2006).
20. Kim A.V., Ryabikin M.Yu., Sergeev A.M. *Usp. Fiz. Nauk*, **169**, 58 (1999).
21. Taranukhin V.D. *Laser Phys*., **10**, 330 (2000).
22. Walser M.W., Keitel C.H., Scrinzi A., Brabec T. *Phys. Rev. Lett*., **85**, 5082 (2000).
23. Emelin M.Yu., Ryabikin M.Yu. *Kvantovaya Elektron*., **43**, 211 (2013) [*Quantum Electron*., **43**, 211 (2013)].
24. Krause J.L., Schafer K.J., Kulander K.C. *Phys. Rev. A*, **45**, 4998 (1992).
25. Emelina A., Emelin M., Ryabikin M. *Techn. Dig. Conf. 'Research in Optical Sciences'* (Berlin, Germany, Optical Society of America, 2014, paper JW2A.19); http://www.opticsinfobase.org/abstract.cfm? URI=HILAS- 2014-JW2A.19.
26. Lewenstein M., Balcou Ph., Ivanov M.Yu., L'Huillier A., Corkum P.B. *Phys. Rev. A*, **49**, 2117 (1994).
27. Salières P., Carré B., Le Déroff L., Grasbon F., Paulus G.G., Walther H., Kopold R., Becker W., Milošević D.B., Sanpera A., Lewenstein M. *Science*, **292**, 902 (2001).
28. Kylstra N.J., Potvliege R.M., Joachain C.J. *J. Phys. B: At. Mol. Opt. Phys*., **34**, L55 (2001).
29. Chirilă C.C., Kylstra N.J., Potvliege R.M., Joachain C.J. *Phys. Rev. A*, **66**, 063411 (2002).

30. Platonenko V.T. *Kvantovaya Elektron*., **31**, 55 (2001) [*Quantum Electron*., **31**, 55 (2001)].
31. Le A.T., Tong X.M., Lin C.D. *Phys. Rev. A*, **73**, 041402(R) (2006).
32. Tong X.M., Lin C.D. *J. Phys. B: At. Mol. Opt. Phys*., **38**, 2593 (2005).
33. Scrinzi A., Geissler M., Brabec T. *Phys. Rev. Lett*., **83**, 706 (1999).
34. Strelkov V.V., Khokhlova M.A., Gonoskov A.A., Gonoskov I.A., Ryabikin M.Yu. *Phys. Rev. A*, **86**, 013404 (2012).